Smartphone-Based Blood Pressure Monitoring via the Oscillometric Finger Pressing Method: Analysis of Oscillation Width Variations Can Improve Diastolic Pressure Computation

Mark Freithaler ⓘ, Anand Chandrasekhar, Vishaal Dhamotharan ⓘ, *Graduate Student Member, IEEE*, Cederick Landry, Sanjeev G. Shroff ⓘ, and Ramakrishna Mukkamala ⓘ, *Senior Member, IEEE*

Abstract—*Objective:* Oscillometric finger pressing is a potential method for absolute blood pressure (BP) monitoring via a smartphone. The user presses their fingertip against a photoplethysmography-force sensor unit on a smartphone to steadily increase the external pressure on the underlying artery. Meanwhile, the phone guides the finger pressing and computes systolic BP (SP) and diastolic BP (DP) from the measured blood volume oscillations and finger pressure. The objective was to develop and evaluate reliable finger oscillometric BP computation algorithms. *Methods:* The collapsibility of thin finger arteries was exploited in an oscillometric model to develop simple algorithms for computing BP from the finger pressing measurements. These algorithms extract features from "width" oscillograms (oscillation width versus finger pressure functions) and the conventional "height" oscillogram for markers of DP and SP. Finger pressing measurements were obtained using a custom system along with reference arm cuff BP measurements from 22 subjects. Measurements were also obtained during BP interventions in some subjects for 34 total measurements. *Results:* An algorithm employing the average of width and height oscillogram features predicted DP with correlation of 0.86 and precision error of 8.6 mmHg with respect to the reference measurements. Analysis of arm oscillometric cuff pressure waveforms from an existing patient database provided evidence that the width oscillogram features are better suited to finger oscillometry. *Conclusion:* Analysis of oscillation width variations during finger pressing can improve DP computation. *Significance:* The study findings may help in converting widely available devices into truly cuffless BP monitors for improving hypertension awareness and control.

Index Terms—Arterial compliance, blood pressure computation, cuffless blood pressure, finger arteries, force sensing, mathematical model, mHealth, oscillometric finger pressing, oscillometry, photoplethysmography (PPG).

I. INTRODUCTION

CUFFLESS blood pressure (BP) measurement could help in improving hypertension awareness and control rates [1]. Studies of cuffless devices are increasingly appearing in the literature [2], and several wearable devices are now cleared by the US Food and Drug Administration or another regulatory body [3], [4], [5], [6], [7], [8], [9].

Most of the studies and likely all of the regulatory-cleared devices at present employ pulse wave analysis (PWA) with or without pulse arrival time (PAT) [1]. PWA methods typically measure a photoplethysmography (PPG) waveform, which indicates distal blood volume oscillations, or a tonometry waveform, which indicates peripheral artery forces, and then apply machine learning to extract features from the waveform and calibrate the features to BP values. PWA-PAT methods operate similarly but also measure an ECG waveform to extract PAT as the time delay between the ECG and hemodynamic waveform and possibly other features.

However, most PWA and PWA-PAT methods require periodic BP measurements with an arm cuff device as part of the calibration procedure and are thus not truly cuffless [3], [4], [5], [6], [7], [8], whereas some of the methods use only individual demographics information but for less reliable calibration [9]. Furthermore, these methods are not directly supported by generally accepted physiological principles. For example, contraction of smooth muscle in small arteries causes the PPG amplitude to vary independently of BP [10], while pre-ejection period (PEP) changes cause PAT to likewise vary independently of BP [11]. As a result, PWA and PWA-PAT methods may not work well. Many studies reporting positive results may actually be misleading [12], and a recent, high-resource study of several PWA and PWA-PAT methods in 1000+ subjects showed that these methods after cuff calibration are essentially of no value in BP measurement [13], [14].
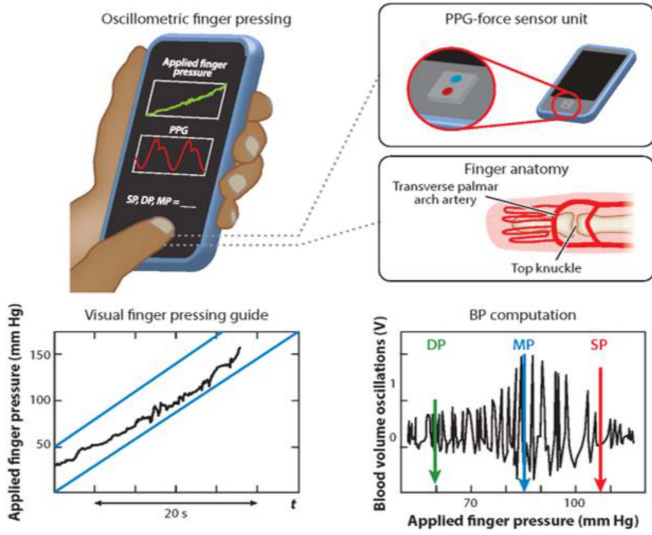
Fig. 1. Oscillometric finger pressing method for cuffless, calibration-free, and principled blood pressure (BP) monitoring via a smartphone. The user presses their fingertip against a photoplethysmography (PPG)-force sensor unit on a smartphone to steadily increase the external pressure of the underlying artery (upper panels), while the phone guides the finger actuation (lower, left panel) and computes systolic BP (SP) and diastolic BP (DP) from the measured blood volume oscillations and finger pressure (lower, right panel). The key challenge is reliable computation of SP and DP. Reproduced from [1].

Oscillometric finger pressing is a different method for cuffless BP measurement [15], [16]. In contrast to the popular methods, this potential method is calibration-free, employs a smartphone, and is based on the same principle as the proven automatic arm cuff device (i.e., oscillometry). The oscillometric principle exploits the sigmoidal blood volume-pressure relationship of arteries. The external pressure of an artery is swept to vary the blood volume oscillation amplitude, and an algorithm is then applied to the oscillation amplitude versus external pressure function (i.e., oscillogram) to compute systolic and diastolic BP (SP and DP). In conventional oscillometry, the cuff is employed to vary the external pressure of the artery and to measure the arterial blood volume oscillations and external pressure via respectively the AC and DC components of the cuff pressure. In the oscillometric finger pressing method, as shown in Fig. 1, the user serves as the actuator instead of the cuff by pressing their fingertip against a smartphone to steadily increase the external pressure of the underlying artery, while the phone acts as the sensor rather than the cuff by employing an embedded PPG-force transducer unit to record the resulting variable-amplitude blood volume oscillations and finger pressure. The phone also visually guides the amount of finger pressure over time and similarly computes SP and DP from the oscillogram. The key outstanding challenge is to compute BP reliably from the finger oscillometric measurements.

In the present study, we developed and evaluated finger oscillometric BP computation algorithms based on physiological modeling. Our most important finding is that analysis of unconventional oscillation width variations during finger pressing can improve the computation of DP.

II. METHODS

A. Finger Oscillometric BP Computation Algorithm Development

We employed a reduced (i.e., parsimonious) oscillometric model [17] to make predictions on finger oscillometric measurements, as shown in Fig. 2. We then developed simple algorithms based on the model predictions, as shown in Fig. 3. The main underlying idea was to exploit a unique aspect of the model parameters for finger arteries compared to the conventional arm (brachial) artery.

Oscillometric Model: The model is based on the sigmoidal blood volume (V)-transmural pressure (P) relationship of arteries (see Fig. 2(a)). Transmural pressure of an artery is defined as the internal BP (P_a) minus the external pressure (P_e). The derivative of the sigmoidal relationship ($f(P)$) with respect to P is the unimodal "arterial compliance curve" ($g(P)$). In oscillometry, $g(P)$ may be well represented with a three-parameter exponential-linear function, where the parameter d denotes the peak amplitude of the curve at zero transmural pressure and the parameters b and c define the negative and positive transmural pressure curve widths [17]. For the brachial artery, $b \approx 11$ mmHg [17]. Hence, this artery is completely occluded only when the external pressure is considerably above SP. In contrast, for the thinner finger arteries, including the transverse palmar arch artery at the fingertip, $b \approx 0$ mmHg. Hence, finger arteries may be fully occluded when the external pressure is just slightly above SP [18]. However, based on previous investigations of the oscillometric finger pressing method [15], [16], we surmise that the ratio c/b may be comparable between the finger and brachial arteries. Hence, we specifically exploited the small b (i.e., collapsibility) of finger arteries.

To complete the model, we assumed that (i) the viscosity of the finger arterial wall can be ignored; (ii) compression of the tissue surrounding the artery during finger pressing can be neglected (because the tissue compression from finger pressing is slow compared to the PPG oscillations); and (iii) PPG oscillations are related to blood volume oscillations via a scale factor k. In this way, the oscillometric model essentially becomes the sigmoidal relationship with the finger BP waveform ($P_a(t)$) at different external pressures (P_e) as input and the varying blood volume waveform ($V(t)$) as output (see Fig. 2(b)). For a slow, linear P_e ramp (due to finger pressing), $V(t)$ oscillates with upper and lower envelopes given by the y-axis reversed sigmoidal relationships evaluated at SP and DP (i.e., $f(P_s - P_e)$ and $f(P_d - P_e)$), respectively (see Fig. 2(c)). High-pass filtering $V(t)$ and scaling by k gives the observed variable PPG oscillations ($O(t)$) during finger pressing (see Fig. 2(d)). Note that the absolute difference of the upper and lower envelopes in $O(t)$ and the absolute difference of the upper and lower envelopes in $V(t)$ are equivalent to within a k scale factor (compare Fig. 2(c) and (d)).

Model Predictions: The model thus indicates that the conventional oscillogram, which is the peak-to-peak amplitude or "height" of the PPG oscillations (O_h) as a function of P_e, is proportional to the difference in the y-axis reversed sigmoidal relationships evaluated at SP and DP (see Fig. 2(e)). From this

(a) $V = f(P)$

Brachial $\cdots$
Finger —

$P = P_a - P_e$

$g(P)$

$g(P) = \dfrac{df(P)}{dP}$

Brachial $\cdots$
Finger —

$P = P_a - P_e$

Exponential-Linear Function:

$$g(P) = d e^{\frac{P}{b}}\left(-\frac{P}{b} + 1\right)u(-P) + d e^{\frac{-P}{c}}\left(-\frac{P}{c} + 1\right)u(P)$$

(b) V

$P_a - P_e$

$P_a(t)$ at different P_e

(c) V

P_e

$f(P_s - P_e)$

$f(P_d - P_e)$

t

(d) $O = kV$

P_e

t

(e) O_h

$P_s = P_{zero}$

$P_{maxslope}$ P_{max} $P_{minslope}$

$$O_h(P_e) = kf(P_s - P_e) - kf(P_d - P_e)$$

(f)

			Brachial	Finger
$P_{maxslope} = P_d - \dfrac{PP}{e^{PP/c} - 1}$			not large	smaller
$P_{minslope} = P_s + \dfrac{PP}{e^{PP/b} - 1}$			not large	smaller
$P_{max} =$	$\dfrac{b}{b+c} P_s +$	$\dfrac{c}{b+c} P_d$	0.4	similar
			0.6	similar

(g) O_w
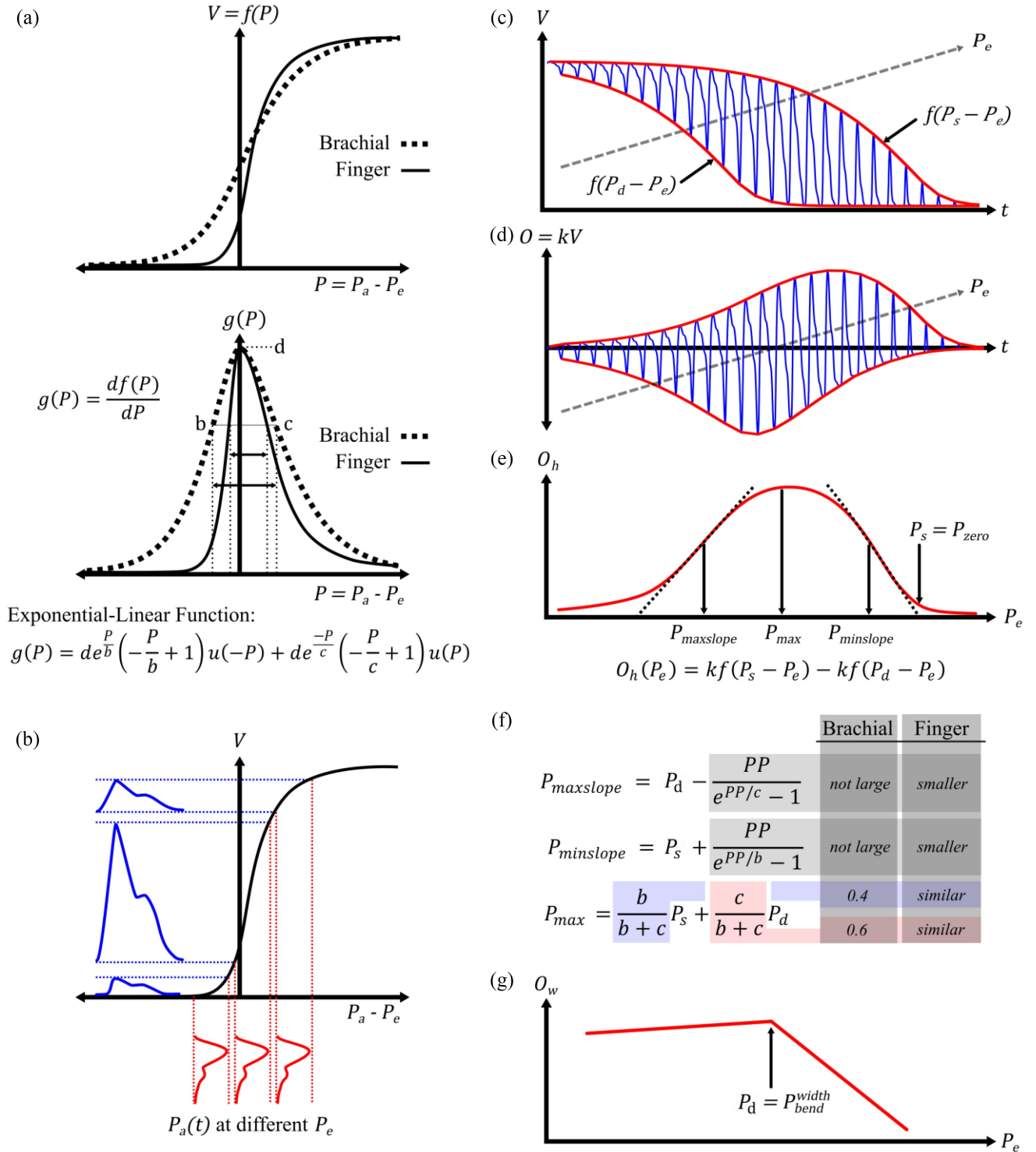
$P_d = P_{bend}^{width}$

P_e

Fig. 2. Oscillometric model and model predictions for computing finger BP from finger oscillometric measurements. (a) Sigmoidal blood volume (V)-transmural pressure (P) relationship of arteries ($f(P)$) upon which the model is based. Transmural pressure of an artery is internal BP (P_a) minus external pressure (P_e); $g(P)$, arterial compliance curve; and $u(\cdot)$, unit step function. Finger but not brachial (arm) arteries are collapsible (i.e., small b parameter). (b) Assumed oscillometric model in which the finger BP waveform ($P_a(t)$) at different P_e is input to $f(P)$ and the varying blood volume waveform ($V(t)$) is output. (c) $V(t)$ in response to a slow, linear P_e ramp (i.e., finger pressing). P_s and P_d are SP and DP. (d) High-pass filtered $V(t)$ scaled by a conversion factor k to model the measured variable PPG oscillations ($O(t)$) during finger pressing. (e) Model for the conventional oscillogram (peak-to-peak amplitude or "height" of the PPG oscillations (O_h) as a function of P_e) arising via comparison of (c) and (d). $P_{maxslope}$, P_{max}, and $P_{minslope}$ are common oscillogram features for computing BP, whereas P_{zero} is an unconventional feature predicted by the model to indicate finger SP. (f) Formulas for $P_{maxslope}$, $P_{minslope}$, and P_{max} via the oscillogram model and the exponential-linear function in (a) [19] predicting that $P_{maxslope}$ and $P_{minslope}$ may be particularly indicative of finger DP and SP. $PP = P_s - P_d$. (g) Model prediction that the unconventional "width" oscillogram (width of the PPG oscillations (O_w) versus P_e) indicates DP via a "bend" therein (P_{bend}^{width}).
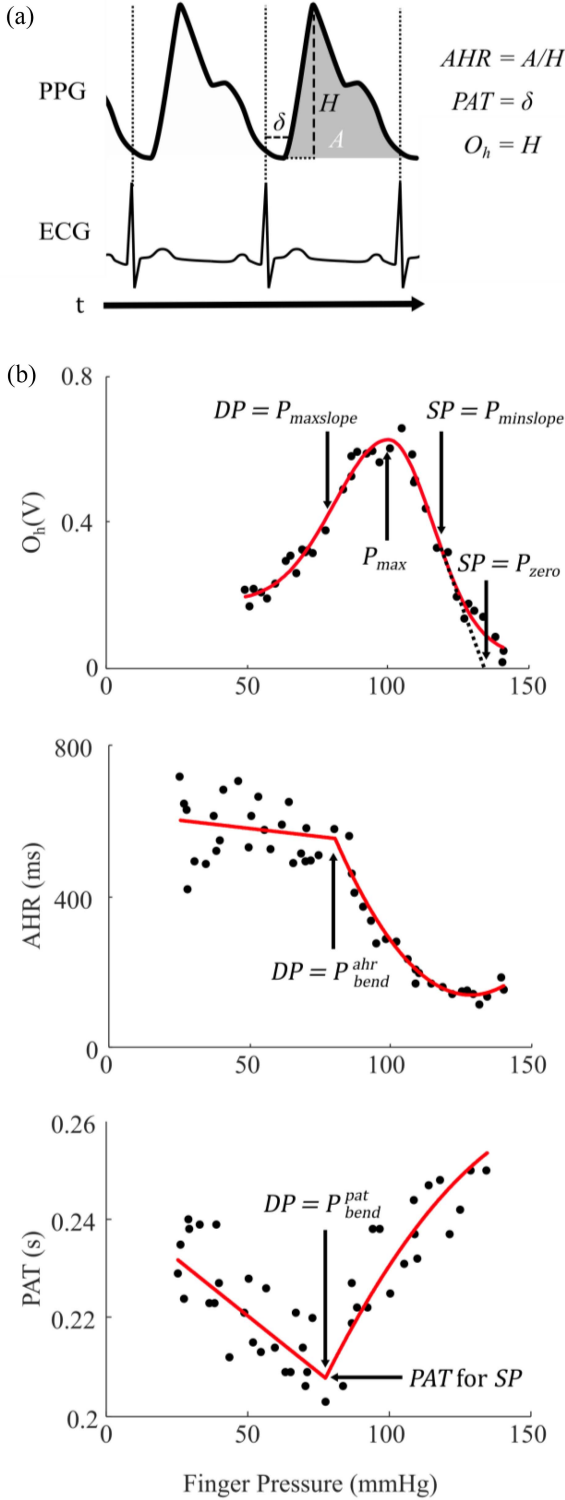
Fig. 3. Model-based algorithms for computing finger BP from finger oscillometric measurements along with a simultaneously acquired ECG waveform. (a) Area to height ratio (AHR) of PPG oscillation and pulse arrival time (PAT, time delay between ECG R-wave and PPG oscillation foot) for quantifying oscillation width. PAT increases with decreasing oscillation width. (b) Height, "AHR," and "PAT" oscillograms and extraction of features therein for computing finger DP and SP as per the model predictions of Fig. 2. P_{bend}^{ahr} and P_{bend}^{pat} are two versions of P_{bend}^{width} in Fig. 2(g); P_{max}, weighted average of DP and SP according to Fig. 2(f); PAT at P_{bend}^{pat}, not based on the model but may offer additive SP information.

oscillogram model with the exponential-linear function for parameterizing $f(P)$ or $g(P)$ therein, formulas for P_e at maximum amplitude (P_{max}), maximum slope ($P_{maxslope}$), and minimum slope ($P_{minslope}$) may be derived (see Fig. 2(f)) [19]. For the brachial artery, the b and c parameter values in the formulas are such that P_{max} occurs at a weighted average of SP and DP (i.e., $0.4P_s + 0.6P_d$), while $P_{maxslope}$ and $P_{minslope}$ occur near DP and SP with errors that are not large (e.g., up to $\sim$8 mmHg for high b and low pulse pressure ($PP = P_s - P_d$) values) [17]. For finger arteries with small b and similar b/c parameter values, $P_{maxslope}$ and $P_{minslope}$ may correspond to DP and SP even more closely, whereas P_{max} may denote a similar weighted average of SP and DP. However, computing slopes is not an artifact-robust operation.

The model also indicates that the widths of the oscillations decrease with increasing P_e (see Fig. 2(d)). Because of the small b in finger arteries, the width reduction begins once P_e exceeds DP (see Fig. 2(b)). Hence, the model specifically predicts that an unconventional "width" oscillogram, which is the width of the PPG oscillations (O_w) versus P_e, indicates DP via a "bend" in the curve (see P_{bend}^{width} in Fig. 2(g)). Such a clear fiducial marker of DP may not be present in the conventional height oscillogram (see Fig. 2(e)). The model with small b further indicates that, when P_e starts to exceed SP, the oscillations will be entirely abolished or identically zero (see Fig. 2(b)). Hence, the model specifically predicts a clear fiducial marker of SP in the height oscillogram of finger arteries (see P_{zero} in Fig. 2(e)).

In sum, the model predicts that (i) $P_{maxslope}$ and P_{bend}^{width} indicate finger DP; (ii) $P_{minslope}$ and P_{zero} indicate finger SP; and (iii) P_{max} indicates a weighted average of finger DP and SP. Since b is not exactly zero, P_{bend}^{width} and P_{zero} may both somewhat overestimate finger DP and SP.

Algorithms: Based on the model predictions, we developed algorithms to compute finger BP from the finger oscillometry measurements as well as a simultaneously acquired ECG waveform. We began by defining oscillation width in two ways: (i) the oscillation area to height ratio (AHR) and (ii) the time delay between the ECG R-wave and oscillation foot (PAT, see Fig. 3(a)). Note that PAT should increase with decreasing oscillation width (see Fig. 2(b)). We then specified seven algorithmic steps with the aid of some preliminary studies as follows:

1) Band-pass filter the PPG (0.3–10 Hz) and ECG (5–15 Hz) waveforms and low-pass filter the finger pressure (0.3 Hz);
2) Identify the R-waves of each beat and utilize the RR intervals to detect the PPG oscillation heights, areas, and feet via the intersecting tangent method [20];
3) Form height, AHR, and PAT beat series and apply objective outlier removal followed by five-beat median filtering to mitigate measurement and respiratory artifacts;
4) Plot the three processed beat series against finger pressure to yield the height oscillogram, "AHR oscillogram", and "PAT oscillogram";
5) Crop (manually) all three oscillograms down to the same finger pressure range to eliminate noisy tails at low and high finger pressures (see Fig. 3(b));

TABLE I
SUMMARY OF FINGER OSCILLOMETRIC BP COMPUTATION ALGORITHMS

BP Computation Algorithm	Feature	Potential Advantage/Disadvantage
DP	$P_{maxslope}$	Closest to DP on average but not noise robust (derivative-based)
	P_{bend}^{pat}	Most robustly detected of DP features but requires ECG
	P_{bend}^{ahr}	Moderate noise robustness without requiring ECG
SP	$P_{minslope}$	Closest to SP on average but not noise robust (derivative-based)
	P_{zero}	Not derivative-based but may still be difficult to detect
	PAT	Additive SP information via ECG but not based on model of Fig. 2
Weighted average of SP and DP	P_{max}	Easiest to detect of all features but does not output SP or DP

See Fig. 3 for all definitions.

6) Fit parametric functions to each oscillogram to further mitigate artifacts as follows: (i) an asymmetric Gaussian function with a left-side offset to the height oscillogram [15]; (ii) a line followed by a concave-up parabola to the AHR oscillogram; and (iii) a line followed by a concave-down parabola to the PAT oscillogram (see Fig. 3(b)); and

7) Analyze the (i) height oscillogram function to detect P_{max}, $P_{maxslope}$, and $P_{minslope}$ per their definitions and P_{zero} as the intersection between the tangent line at $P_{minslope}$ and the x-axis and (ii-iii) AHR and PAT oscillogram functions to detect their bends (P_{bend}^{ahr} and P_{bend}^{pat}), via the intersection between their respective lines and parabolas, as well as the PAT at P_{bend}^{pat} (i.e., fixed transmural pressure), which could provide some additive SP information [10] (see Fig. 3(b)).

In sum, the algorithms extracted seven, mainly physiological model-based features with potential relationship to finger SP and DP from the finger PPG waveform, finger pressure, and an ECG waveform during finger pressing. Notably, the features constitute main fiducial markers in height and width oscillograms. The algorithms may thus be regarded as simple and possibly afford lower BP error variance than more complicated algorithms in which finer or detailed features are targeted. Table I summarizes the features and their potential advantage and disadvantage relative to each other.

B. Algorithm Evaluation

We evaluated the simple algorithms against reference cuff BP measurements in a group of volunteers. The human study was approved by the University of Pittsburgh IRB (STUDY20060267, 2020 –), and all study subjects provided written, informed consent.

We recruited 22 healthy volunteers. Their demographics were as follows: 50% female, 39±11 (mean±SD) years, 73±10 kg, and 172±8 cm.

We utilized our previously built custom benchtop system for implementing the oscillometric finger pressing method [21]. The system is illustrated in Fig. 4(a) and includes (i) a hand-held device comprising an infrared reflectance-mode LED and photodetector pair on top of a load cell to measure finger PPG oscillations and pressure; (ii) electrodes in lead I configuration to measure an ECG waveform; (iii) a computer display to visually guide the finger pressing; and (iv) a commercial data acquisition unit (USB-6003, NI) to record the data. As shown in Fig. 4(b), we further employed a volume-clamp device (Nexfin, BMEYE) to obtain finger cuff BP and an oscillometric device (BP7100, Omron) to measure arm cuff BP.

We began by explaining how to implement the oscillometric finger pressing method with the benchtop system as well as making cuff BP measurements to acclimate the subjects to the study. Each study subject then performed serial oscillometric finger pressing trials with the custom device held at heart level until two high-quality measurements were made per visual inspection. A study subject performed about seven trials on average. We then obtained two successive arm cuff BP measurements with the oscillometric device and a finger cuff BP measurement with the volume-clamp device. All individual measurements were made at least one minute apart. As shown in Fig. 4(c), four study subjects who were experienced in implementing the oscillometric finger pressing method repeated these procedures with the custom and volume-clamp devices held well above and well below heart level to substantially lower and raise their finger BP by calculable amounts (i.e., $\rho g h$, where ρ is the known blood density, g is gravity, and h is the measured vertical distance between the device and heart level). As also shown in Fig. 4(c), these four study subjects additionally performed 50 squats to appreciably increase their PP, remained at rest for another minute, and then performed a single oscillometric finger pressing trial while receiving a concurrent arm cuff BP measurement.

We applied the algorithms to each of the high-quality finger pressing measurements to compute P_{bend}^{ahr}, P_{bend}^{pat}, $P_{maxslope}$, $P_{minslope}$, P_{zero}, PAT at P_{bend}^{pat}, and P_{max}. We normalized the PAT feature by the height of the study subject and took the reciprocal to assess height/PAT. We then averaged all pairs of features as well as cuff BP measurements to arrive at a total of 34 measurement sets from 22 study subjects.

We found that the seven features extracted by the algorithms from the finger pressing measurements correlated noticeably better with the arm cuff BP measurements than the finger cuff BP measurements. Since agreement with arm cuff BP is the main goal of cuffless devices, we decided to use arm cuff BP as the sole reference measurement in this study. It is therefore important to note that finger DP is smaller than arm DP by about 10 mmHg due to a resistive BP drop between the arm and finger arteries [22]. Meanwhile, finger and arm SP may be more variably related due to arterial wave reflection-induced amplification of PP with increasing distance from the heart [22]. We first added $\rho g h$ to the arm cuff SP and DP to yield reference measurements for the "hydrostatic" interventions in which the devices were held above or below heart level. Then, we evaluated each feature against reference arm cuff SP and DP
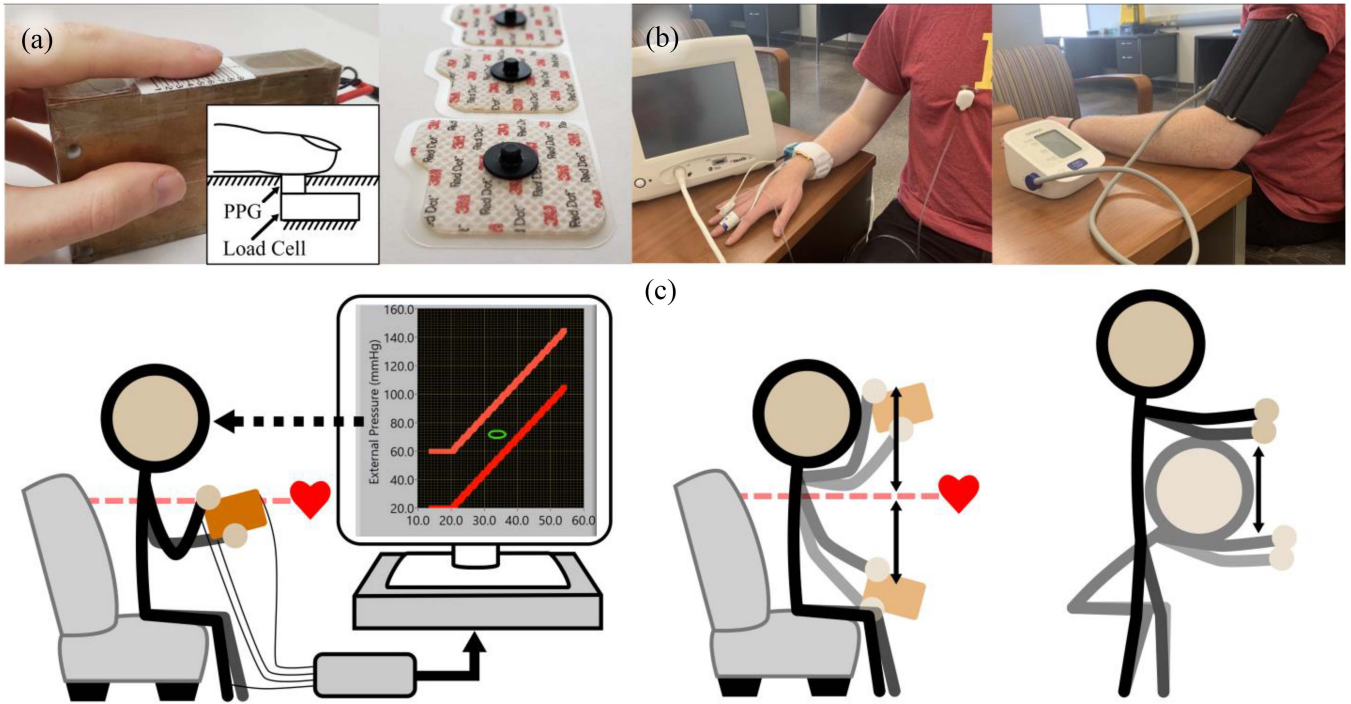
Fig. 4. Algorithm evaluation. (a) Custom benchtop system for recording oscillometric finger pressing measurements and simultaneously acquiring an ECG waveform [21]. (b) Volume-clamp device for obtaining reference finger cuff BP and a standard oscillometric device for measuring reference arm cuff BP. The arm cuff device appeared more reliable than the volume-clamp device. (c) Maneuvers performed by a subset of study subjects to change BP.

via correlation analysis. To mitigate the impact of finger and arm BP differences and explore combinations of features, we also trained linear regression equations to predict arm cuff BP from select features. We tested the agreement between the predicted and arm cuff BP via correlation and Bland-Altman analyses. We applied leave-one-out cross validation for this evaluation.

III. RESULTS

Fig. 5(a) to (c) illustrate a representative example of a raw finger pressing measurement from a study subject and the associated height and AHR oscillograms constructed from the same measurement over the entire finger pressure range, respectively. The blue and red vertical lines here denote the times of the ECG R-waves and oscillation feet and thereby illustrate PAT. As indicated by this example, the model predictions generally agreed with the measurements in that the PPG oscillation height increased and then decreased, while the oscillation width decreased, with increasing finger pressure (compare Fig. 2(d) with Figs. 5(a), 2(e) with 5(b), and Figs. 2(g) to 5(c)). However, the model predictions generally disagreed with the measurements at low and high finger pressures (compare Figs. 2(e) with 5(b)). At low finger pressures, the measured oscillograms revealed substantial oscillations of approximately constant amplitude or inverted U-shape. These oscillations likely arose from the smaller vessels in the fingertip (e.g., arterioles and capillaries), which were ignored by the model. At high finger pressures, the measured oscillograms likewise indicated appreciable oscillations and a gradual decaying tail in particular. These oscillations

possibly arose from arterial pulsations proximal to the occluded artery, which were also neglected by the model. Importantly, the algorithms extract features primarily from the measurements around the peak oscillation rather than at low or high finger pressures.

The reference arm cuff DP and SP ranged from 37 to 110 and 84 to 152 mmHg (34 measurements from 22 study subjects). The extrema causing these wide BP ranges were attained via hydrostatic and exercise interventions performed by some of the study subjects. The correlation between the arm cuff DP and SP measurements was high ($r = 0.85$). Hence, each feature extracted by the algorithms from the finger pressing measurements was expected to show comparable correlations with the reference DP and SP.

Fig. 6 shows correlations plots of each of the seven features versus arm cuff DP (blue data points) and SP (red data points). Consistent with the model predictions, $P_{maxslope}$, P_{bend}^{ahr}, and P_{bend}^{pat} indicated DP better than SP, as the DP datapoints (blue) were closer to the identity line than the SP datapoints (red). The blue datapoints were on the identity line for P_{bend}^{ahr} and P_{bend}^{pat} due to the finger DP overestimation by these features offsetting higher arm DP than finger DP and were below the identity line for $P_{maxslope}$ due to the minimal finger DP bias error via this feature together with finger DP being lower than arm DP. $P_{maxslope}$, P_{bend}^{ahr}, and P_{bend}^{pat} showed solid correlations with DP ($r = 0.79$–0.81) as well. As expected and congruent with the model predictions, $P_{minslope}$ and P_{zero} indicated SP better than DP, as the SP datapoints (red) were closer to the identity line than the DP datapoints (blue). The red datapoints were
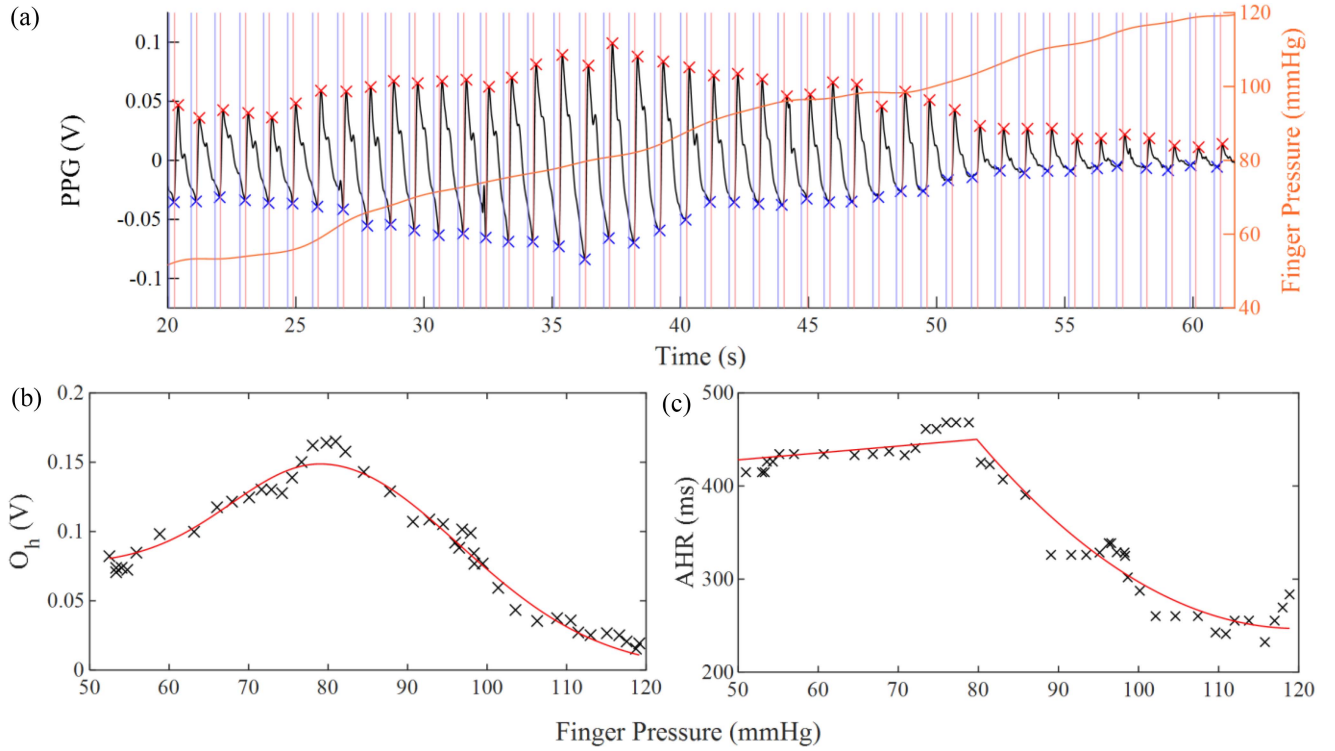
Fig. 5. Representative example of oscillometric finger pressing measurements over the entire finger pressing range from a study subject. (a) Raw measurements comprising PPG oscillations and finger pressure, with blue and red vertical lines denoting the times of the ECG R-waves and oscillation feet and thus PAT. (b) Conventional oscillogram derived from the same measurements. (c) AHR oscillogram derived from the measurements (see Fig. 3).
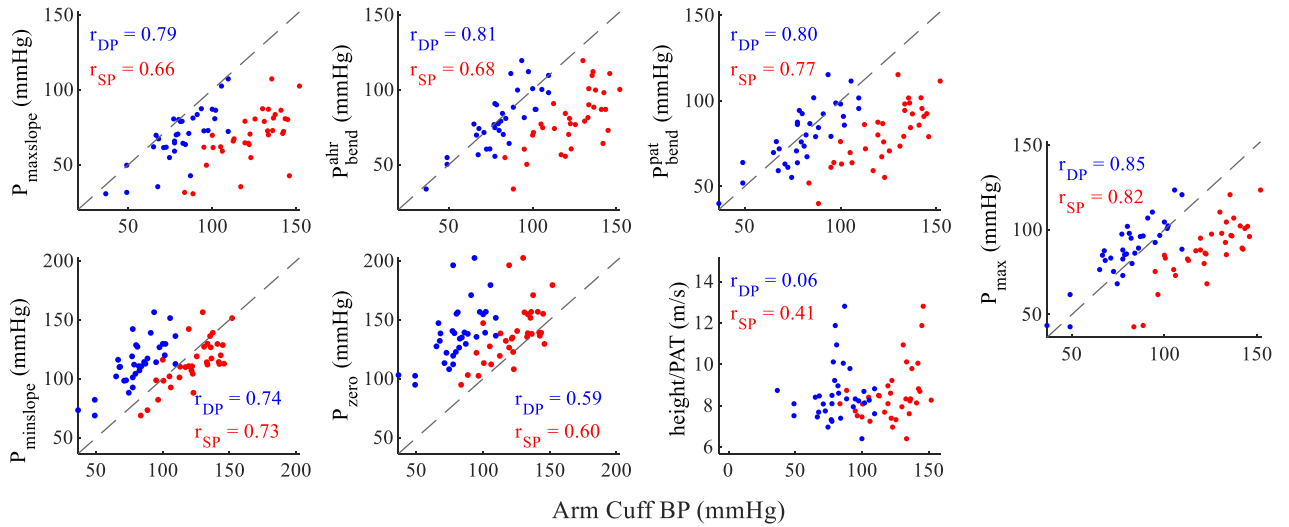

Fig. 6. Correlations plots of each of the features extracted by the algorithms versus arm cuff DP (blue data points) and SP (red data points) overall (34 measurements from 22 study subjects). Height is study subject height; r, correlation coefficient; and dashed line, line of identity.

higher for P_{zero} than $P_{minslope}$ by definition (see Fig. 3(b)). However, $P_{minslope}$ yielded correlation with SP (r = 0.73) that was noticeably better than P_{zero}. Height/PAT, which was not a physiological model-based feature, showed some correlation with SP (r = 0.41) but not DP. This modest correlation may represent additive information to the model-based features. Also

consistent with the model predictions, P_{max} overestimated DP (even though arm DP is higher than finger DP) and underestimated SP, thereby indicating that it may be a comparably weighted average of the two BP values. P_{max} correlated with both DP and SP better than any of the other features (r = 0.85 and 0.82) just because it was the most robustly identified feature.

Fig. 7(a) shows leave-one-out predicted DP via linear regression with $P_{maxslope}$, P_{bend}^{ahr}, P_{bend}^{pat}, and the average of these three features as sole inputs versus arm cuff DP, while Fig. 7(b) shows leave-one-out predicted SP via linear regression with $P_{minslope}$ alone as input and $P_{minslope}$ and height/PAT as dual inputs versus arm cuff SP. The predicted DP via the average of $P_{maxslope}$, P_{bend}^{ahr}, and P_{bend}^{pat} yielded the highest correlation with reference DP (r = 0.86 compared to 0.75–0.77 for the three individual features) and lowest precision error against the reference DP (σ = 8.6 mmHg compared to 10.8–11.2 mmHg for the three individual features). The inclusion of height/PAT as a second feature to $P_{minslope}$ improved the SP prediction (r = 0.75 and σ = 11.9 mmHg). However, the precision error for SP was still relatively high. It is important to note that these predictions constitute independent measurement of SP and DP and do not trivially leverage the high correlation between arm cuff DP and SP in the study subjects.

IV. Discussion

A. Summary

The oscillometric finger pressing method could potentially permit truly cuffless BP monitoring via widely available smartphones (see Fig. 1) [15], [16]. However, reliable computation of BP from the measured finger PPG oscillations and finger pressure remains a key challenge. We employed a reduced mathematical model of oscillometry [17] and exploited the collapsibility of thin finger arteries [18] (see Fig. 2) to develop simple algorithms for computing BP from the finger pressing measurements including a simultaneously acquired ECG waveform (see Fig. 3 and Table I). We evaluated the algorithms against reference arm cuff BP measurements at baseline in a group of study subjects and during interventions to change BP in a subset of the study subjects with experience in implementing the method (see Fig. 4). Our most important finding was that analysis of oscillation width variations during finger pressing (see Fig. 5) can improve the computation of DP (see Figs. 6 and 7).

B. Diastolic Pressure (DP) Computation Algorithms

We constructed unconventional "width" oscillograms (i.e., oscillation width versus finger pressure functions) by defining width in two ways: (i) the oscillation area to height ratio (AHR) and (ii) pulse arrival time (PAT, time delay between ECG R-wave and oscillation foot). We then detected the "bends" in the "AHR oscillogram" and "PAT oscillogram" (P_{bend}^{ahr} and P_{bend}^{pat}) as markers of DP (see Fig. 3). We also constructed the conventional "height" oscillogram and then identified the finger pressure at maximum slope ($P_{maxslope}$) for another DP marker (see Fig. 3). Although this third feature is well-known in traditional arm cuff oscillometry, our modeling of collapsible finger arteries here suggested that it is better suited for finger than arm arteries (see Fig. 2(f)). We showed that the average of $P_{maxslope}$, P_{bend}^{ahr}, and P_{bend}^{pat} could predict DP the best, with correlation of 0.86 and precision error of 8.6 mmHg against the reference arm cuff device over a sizeable DP range (see Fig. 7).

For benchmarking purposes, the well-known standard precision error limit is 8 mmHg. However, it should be noted that we did not employ a standard evaluation protocol, which is resource intensive.

Oscillation width variation features as markers of DP are relatively unknown in oscillometric BP computation. Firstly, while longstanding finger cuff volume-clamp devices employ finger oscillometry to determine the PPG setpoint, only mean BP is effectively detected in this initialization step [1]. Secondly, the thicker arm (brachial artery) is hard to collapse, so oscillation width variation features may be less effective in standard arm cuff oscillometry. To verify this latter assertion, we analyzed an existing cardiac catheterization patient database comprising oscillometric arm cuff pressure, ECG, and reference invasive brachial BP waveforms (195 measurements from 122 patients) [23], [24]. Fig. 8(a) shows examples of the constructed AHR and PAT oscillograms. The AHR oscillograms did not reveal the expected shape (e.g., concave-down pattern) in 22 of 195 measurements, while the PAT oscillograms were more inconsistent in shape (and in fact rarely showed a concave-down pattern as reported in an earlier study [25]). Fig. 8(b) shows that P_{bend}^{ahr} detected from the 173 AHR oscillograms, which had the expected shape, did not agree well with reference DP or SP. Because this database did not include finger pressing measurements, we could not directly compare the performance of arm and finger width oscillograms in tracking BP. We therefore conducted a small exploratory study wherein the oscillometric arm cuff pressure waveform was first recorded using a modified arm cuff device and then finger pressing measurements were obtained as described above in five subjects. Fig. 8(c) shows that arm P_{bend}^{ahr} did not agree with arm cuff DP as well as finger P_{bend}^{ahr} and finger P_{bend}^{pat}. Hence, oscillation width variation features may indeed be particularly suited to finger oscillometry.

C. Systolic Pressure (SP) Computation Algorithms

We also analyzed the height oscillogram to detect the finger pressures at minimum slope ($P_{minslope}$) and at subsequent zero oscillations (P_{zero}) as markers of SP (see Fig. 3). Similarly, the $P_{minslope}$ feature is well-known but may be better suited for finger than arm arteries (see Fig. 2(f)). We further detected the height/PAT value at P_{bend}^{pat} in the PAT oscillogram for a third marker of SP (see Fig. 3). PAT is not a physiological model-based feature but may offer some additive SP information [10]. Although PAT values are affected by the PPG sensor contact pressure on the skin [21], this confounding effect was eliminated here by virtue of always detecting PAT near zero transmural pressure (i.e., at P_{bend}^{pat}). We showed that $P_{minslope}$ and height/PAT could together predict SP with correlation of 0.75 and precision error of 11.9 mmHg against the reference arm cuff device (see Fig. 7). The P_{zero} feature did not track SP as well (see Fig. 6), because the height oscillograms often showed a gradually decaying tail at high finger pressure, which obscured the detection of this feature. This tail may possibly have been caused by proximal arterial pulsations and were not considered in the modeling. These P_{zero} findings are at odds
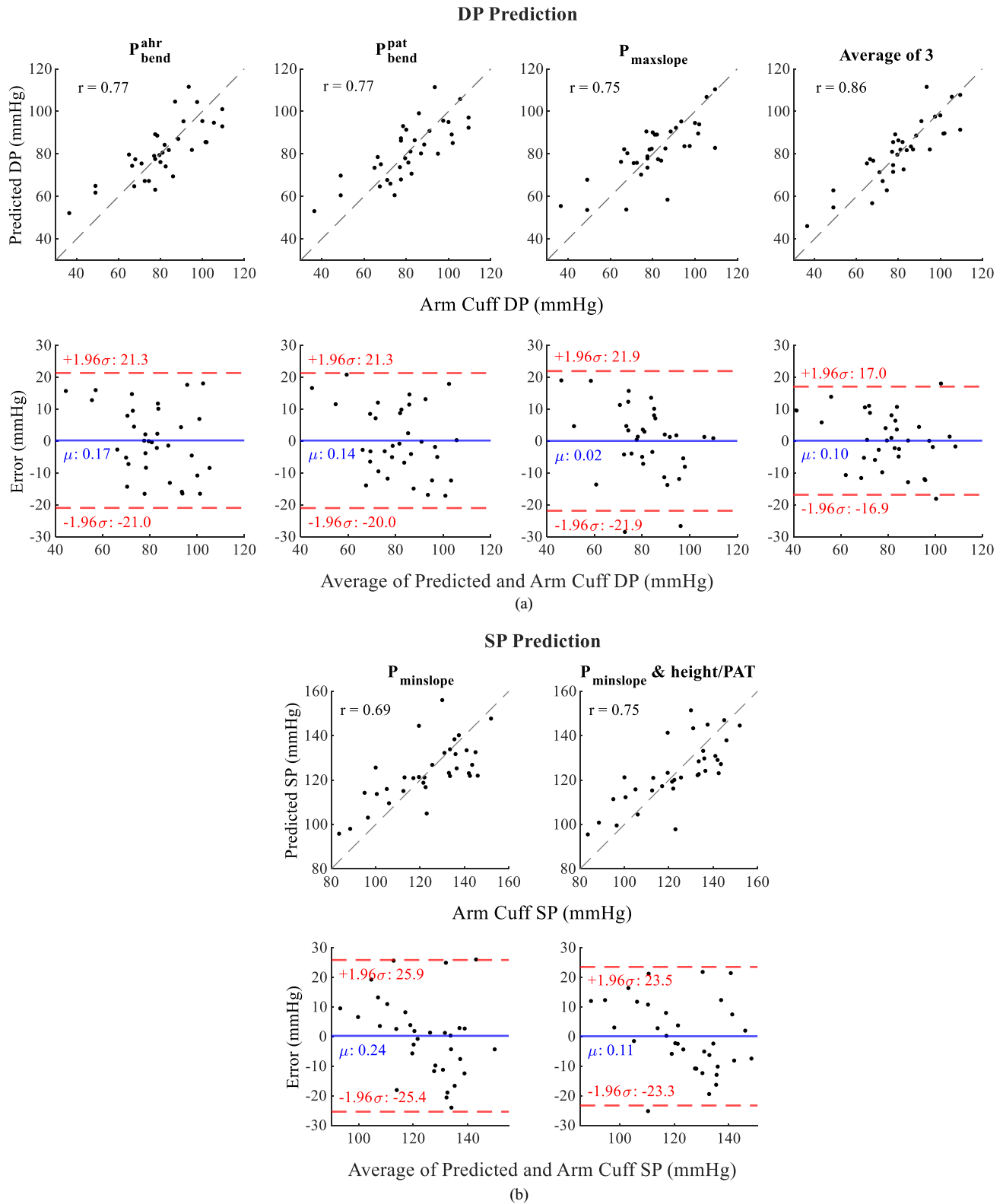
Fig. 7. Correlation and Bland–Altman plots of leave-one-out predicted BP from select features versus arm cuff BP overall (34 measurements from 22 study subjects). (a) Predicted DP results via linear regression with $P_{maxslope}$, P_{bend}^{ahr}, P_{bend}^{pat}, and the average of these three features as sole inputs. μ is bias error (mean of errors) and σ, precision error (SD of errors). (b) Predicted SP results via linear regression with $P_{minslope}$ alone as input and $P_{minslope}$ and height/PAT as dual inputs.
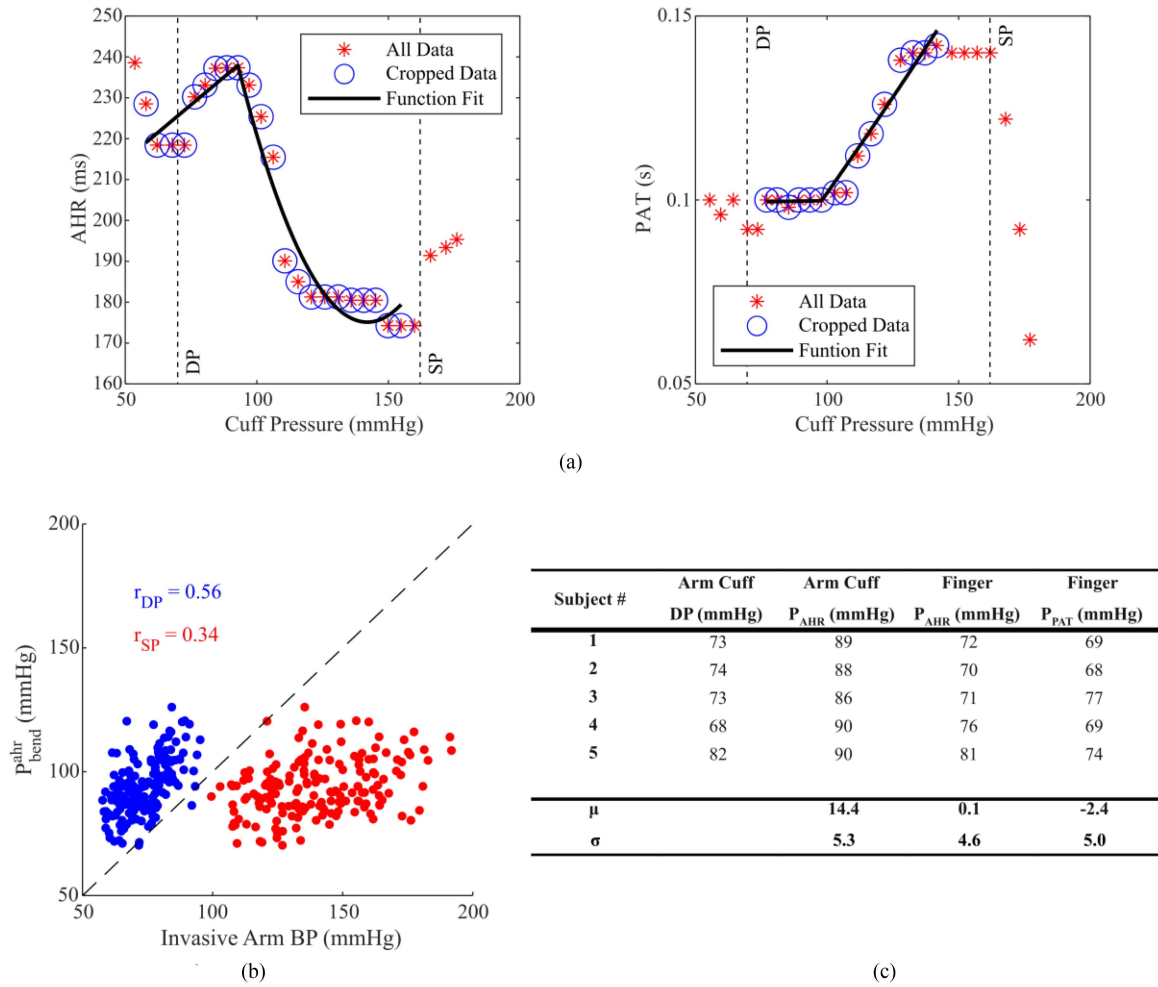
(a)

(b)

Subject #	Arm Cuff DP (mmHg)	Arm Cuff P_{AHR} (mmHg)	Finger P_{AHR} (mmHg)	Finger P_{PAT} (mmHg)
1	73	89	72	69
2	74	88	70	68
3	73	86	71	77
4	68	90	76	69
5	82	90	81	74
μ		14.4	0.1	-2.4
σ		5.3	4.6	5.0

(c)

Fig. 8.   Evaluation of P^{ahr}_{bend} and P^{pat}_{bend} detected from oscillometric arm cuff pressure waveforms as markers of BP. (a) Example AHR and PAT oscillograms from an oscillometric arm cuff pressure waveform of a patient in an existing database (195 measurements from 122 patients) [23], [24]. The PAT oscillogram shapes were relatively inconsistent compared to the AHR oscillogram shapes overall. (b) P^{ahr}_{bend} detected from the 173 AHR oscillograms, which had the expected shape, versus invasive reference arm DP or SP. (c) Comparison of arm cuff P^{ahr}_{bend} versus finger P^{ahr}_{bend} and P^{pat}_{bend} using arm cuff DP as a reference (five subjects).

with a previous finger oscillometry study showing that a similar feature could tightly agree with SP [26]. That study used a finger cuff-transmissive-mode PPG system for the digital arteries and invasive reference brachial BP. It is also important to note that the previous study did not propose any algorithm to compute DP [26].

There are several reasons that the finger BP computation algorithms did not agree with arm cuff SP as well as arm cuff DP. One reason is that the derivative operation needed to detect $P_{minslope}$ is well-known to amplify measurement artifact. While the same can be said for $P_{maxslope}$, derivative-induced error was mitigated by averaging this feature with the oscillation width variation features (see Fig. 7). Another reason is that the automatic arm cuff device, which was utilized here as the reference, is less accurate in measuring arm SP than arm DP [23], [27]. A third reason is that the difference between finger and arm SP is more variable than finger and arm DP [22]. In finger cuff volume-clamp devices, a transfer function is typically used to reduce the arterial wave reflection-induced PP amplification at

the finger compared to the arm [22]. However, such a transfer function was not applicable in this study, because the computed finger PP was lower than arm cuff PP on average (results not shown). For this reason, we resorted to straightforward linear regression to attempt to reduce finger and arm BP differences. The underestimation of PP here may be due to neglecting the viscosity of the arterial wall in the model.

D. Maximum Amplitude Algorithm for Computing a Weighted Average of SP and DP

We additionally analyzed the height oscillogram to detect the finger pressure at maximum amplitude (P_{max}). According to our physiological model (see Fig. 2(f)), P_{max} is a weighted average of SP and DP, where the weightings are given by the arterial compliance curve widths over the negative (b) and positive (c) transmural pressure ranges. Our DP computation results indicate that b is smaller for finger than arm arteries but say little about c. If c were similar for finger and arm arteries, then P_{max} should

equate to finger DP based on the model. However, we found that P_{max} was higher than arm cuff DP, which again is about 10 mmHg higher than finger DP (see Fig. 6). This result is consistent with our prior work on the oscillometric finger pressing method [15], [16]. Hence, the ratio of arterial compliance curve widths over the negative and positive transmural pressure ranges (i.e., b/c) may in fact be similar in finger and arm arteries, and P_{max} may be a comparably weighted average of DP and SP for both arteries. Note that the robustly detected and most popular P_{max} feature showed the strongest correlation with arm cuff DP and SP (see Fig. 6) merely because DP and SP were highly correlated in this study.

E. Incorporating ECG With Oscillometric Finger Pressing

As we have described, we incorporated ECG measurement in the oscillometric finger pressing method here. The PAT oscillograms showed concave-up patterns (see Fig. 3), which confirmed our prior work on assessing the impact of PPG sensor contact pressure on finger PAT [21]. However, the PAT oscillograms here are in stark contrast to an earlier study on the impact of PPG sensor contact pressure on PAT that reported concave-down patterns [28]. Overall, we found that PAT did not help much in BP computation. In particular, averaging only $P_{maxslope}$ and P_{bend}^{ahr} could predict DP with correlation of 0.86 and precision error of 8.8 mmHg, which is comparable to including P_{bend}^{pat} in the average (see Fig. 7). While using height/PAT with $P_{minslope}$ did reduce the SP precision error by $\sim$9% compared to using $P_{minslope}$ alone (see Fig. 7), this improvement was driven by the exercise intervention (see red datapoints with higher height/PAT values in Fig. 6) and may not generalize to other types of BP changes [1]. Even so, PAT is easily detectable and it is still possible that it could be of value in computing BP in lower signal-to-noise conditions. An ECG waveform is also helpful for detecting heartbeats and arrhythmias. Hence, ECG could still prove important in the context of the oscillometric finger pressing method.

F. Limitations

Our study has some limitations. Firstly, we used an automatic arm cuff device as the reference. Such devices are not as accurate as manual auscultation (performed by an expert) in measuring arm BP. Furthermore, the model-based algorithms compute finger BP from the finger pressing measurement rather than arm BP. We did try to use a finger cuff volume-clamp device for reference finger BP measurements. However, the BP computed by the algorithms correlated better with more relevant arm cuff BP. Note that finger cuff volume-clamp devices have never been validated for finger BP measurement due to a lack of a reference, but several are FDA-cleared for measuring arm BP measurement. Secondly, arm cuff SP and DP in our study subjects showed high correlation (r = 0.85). We did try to mitigate the correlation somewhat by invoking exercise in a subset of study subjects. We also explored only independent computation of SP and DP rather than trivially leveraging the high correlation to report misleadingly good SP computation results. However, in general, SP and DP are correlated (e.g., r = 0.7) [29], [30]. So, it would seem reasonable for SP and DP features to overlap rather than be mutually exclusive. Using multiple features was difficult though due to feature collinearity arising from the high SP and DP correlation. Thirdly, we did not precisely control for correct fingertip and heart level positioning by the study subjects. These three limitations surely contributed to the BP computation errors reported herein. Future studies should focus on addressing these limitations with the goal of further reducing the BP computation errors. It is also worth mentioning that the standard error limits for the oscillometric finger pressing method could potentially be relaxed (e.g., SP precision error limit from 8 to even $\sim$12 mmHg) due to the capability of making many measurements over time with the method [31].

V. CONCLUSION

We investigated the oscillometric finger pressing method for potential cuffless and calibration-free BP monitoring via widely available smartphones. We specifically developed simple algorithms based on physiological modeling of finger arteries for computing BP from the measured variable finger PPG oscillations and finger pressure and evaluated the algorithms against an automatic arm cuff device in healthy study subjects and during some interventions to change BP. Our most important finding was that analysis of unconventional oscillation width variations versus finger pressure can improve the computation of DP. Future studies should confirm this finding in diverse people using manual auscultation as the reference. Additional work is needed to conceive finger oscillometric algorithms for more reliably computing SP. With successful ensuing research, smartphone-based BP monitoring via the oscillometric finger pressing method may uniquely help in improving hypertension awareness and control rates.

ACKNOWLEDGMENT

REFERENCES

[1] R. Mukkamala, G. S. Stergiou, and A. P. Avolio, "Cuffless blood pressure measurement," *Annu. Rev. Biomed. Eng.*, vol. 24, pp. 203–230, 2022, doi: 10.1146/annurev-bioeng-110220-014644.

[2] "NCBI PubMed search," *National Library of Medicine*, Apr. 2023. Accessed: Apr. 10, 2023. [Online]. Available: https://pubmed.ncbi.nlm.nih.gov/?term=cuffless+OR+cuff-less+AND+blood+AND+pressure&filter=years.1960-2023&timeline=expanded

[3] T. Tamura, "Regulation and approval of continuous, non-invasive blood-pressure monitoring devices," in *IFMBE Proceedings MEDICON*, J. Henriques, Ed. Berlin, Germany: Springer, 2020, pp. 1021–1027, doi: 10.1007/978-3-030-31635-8.

[4] D. Nachman et al., "Twenty-four-hour ambulatory blood pressure measurement using a novel noninvasive, cuffless, wireless device," *Amer. J. Hypertension*, vol. 34, no. 11, pp. 1171–1180, Nov. 2021, doi: 10.1093/ajh/hpab095.

[5] J. Sola et al., "Guidance for the interpretation of continual cuffless blood pressure data for the diagnosis and management of hypertension," *Front. Med. Technol.*, vol. 4, 2022, Art. no. 899143. [Online]. Available: https://www.frontiersin.org/articles/10.3389/fmedt.2022.899143

[6] A. Vybornova et al., "Blood pressure from the optical Aktiia bracelet: A 1-month validation study using an extended ISO81060-2 protocol adapted for a cuffless wrist device," *Blood Press. Monit.*, vol. 26, pp. 305–311, 2021, doi: 10.1097/MBP.0000000000000531.

[7] J. H. Ahn et al., "Validation of blood pressure measurement using a smartwatch in patients with Parkinson's disease," *Front. Neurol.*, vol. 12, 2021, Art. no. 650929. [Online]. Available: https://www.frontiersin.org/articles/10.3389/fneur.2021.650929

[8] D. Nair et al., "The use of ambulatory tonometric radial arterial wave capture to measure ambulatory blood pressure: The validation of a novel wrist-bound device in adults," *J. Hum. Hypertension*, vol. 22, no. 3, pp. 220–222, 2008, doi: 10.1038/sj.jhh.1002306.

[9] G. Sayer et al., "Continuous monitoring of blood pressure using a wrist-worn cuffless device," *Amer. J. Hypertension*, vol. 35, no. 5, pp. 407–413, May 2022, doi: 10.1093/ajh/hpac020.

[10] K. Natarajan et al., "Photoplethysmography fast upstroke time intervals can be useful features for cuff-less measurement of blood pressure changes in humans," *IEEE Trans. Biomed. Eng.*, vol. 69, no. 1, pp. 53–62, Jan. 2022, doi: 10.1109/TBME.2021.3087105.

[11] M. Gao, N. B. Olivier, and R. Mukkamala, "Comparison of noninvasive pulse transit time estimates as markers of blood pressure using invasive pulse transit time measurements as a reference," *Physiol. Rep.*, vol. 4, no. 10, pp. 1–7, 2016, doi: 10.14814/phy2.12768.

[12] R. Mukkamala et al., "Evaluation of the accuracy of cuffless blood pressure measurement devices: Challenges and proposals," *Hypertension*, vol. 78, pp. 1161–1167, 2021, doi: 10.1161/HYPERTENSIONAHA.120.14719.

[13] R. Mieloszyk et al., "A comparison of wearable tonometry, photoplethysmography, and electrocardiography for cuffless measurement of blood pressure in an ambulatory setting," *IEEE J. Biomed. Health Inform.*, vol. 26, no. 7, pp. 2864–2875, Jul. 2022, doi: 10.1109/JBHI.2022.3153259.

[14] R. Mukkamala et al., "The microsoft research aurora project: Important findings on cuffless blood pressure measurement," *Hypertension*, vol. 80, no. 3, pp. 534–540, 2023, doi: 10.1161/HYPERTENSIONAHA.122.20410.

[15] A. Chandrasekhar et al., "Smartphone-based blood pressure monitoring via the oscillometric finger-pressing method," *Sci. Transl. Med.*, vol. 10, no. 431, pp. 1–12, 2018, doi: 10.1126/scitranslmed.aap8674.

[16] A. Chandrasekhar et al., "An iPhone application for blood pressure monitoring via the oscillometric finger pressing method," *Sci. Rep.*, vol. 8, no. 13136, pp. 1–6, 2018, doi: 10.1038/s41598-018-31632-x.

[17] V. Dhamotharan et al., "Mathematical modeling of oscillometric blood pressure measurement: A complete, reduced oscillogram model," *IEEE Trans. Biomed. Eng.*, vol. 70, no. 2, pp. 715–722, Feb. 2023, doi: 10.1109/TBME.2022.3201433.

[18] G. J. Langewouters et al., "Pressure-diameter relationships of segments of human finger arteries," *Clin. Phys. Physiol. Meas.*, vol. 7, no. 1, pp. 43–55, 1986, doi: 10.1088/0143-0815/7/1/003.

[19] A. Chandrasekhar et al., "Formulas to explain popular oscillometric blood pressure estimation algorithms," *Front. Physiol.*, vol. 10, no. 1415, pp. 1–14, 2019, doi: 10.3389/fphys.2019.01415.

[20] Y. C. Chiu et al., "Determination of pulse wave velocities with computerized algorithms," *Amer. Heart J.*, vol. 121, no. 5, pp. 1460–1470, 1991.

[21] A. Chandrasekhar et al., "PPG sensor contact pressure should be taken into account for cuff-less blood pressure measurement," *IEEE Trans. Biomed. Eng.*, vol. 67, no. 11, pp. 3134–3140, Nov. 2020, doi: 10.1109/TBME.2020.2976989.

[22] P. Gizdulich, A. Prentza, and K. H. Wesseling, "Models of brachial to finger pulse wave distortion and pressure decrement," *Cardiovasc. Res.*, vol. 33, no. 3, pp. 698–705, 1997, doi: 10.1016/S0008-6363(97)00003-5.

[23] J. Liu et al., "Patient-specific oscillometric blood pressure measurement: Validation for accuracy and repeatability," *IEEE J. Transl. Eng. Health Med.*, vol. 5, 2017, Art. no. 1900110, doi: 10.1109/JTEHM.2016.2639481.

[24] H.-M. Cheng et al., "Measurement accuracy of a stand-alone oscillometric central blood pressure monitor: A validation report for microlife watch BP office central," *Amer. J. Hypertension*, vol. 26, no. 1, pp. 42–50, Jan. 2013, doi: 10.1093/ajh/hps021.

[25] M. Forouzanfar et al., "Coefficient-free blood pressure estimation based on pulse transit time–cuff pressure dependence," *IEEE Trans. Biomed. Eng.*, vol. 60, no. 7, pp. 1814–1824, Jul. 2013, doi: 10.1109/TBME.2013.2243148.

[26] K. Yamakoshi et al., "New oscillometric method for indirect measurement of systolic and mean arterial pressure in the human finger. Part 2: Correlation study," *Med. Biol. Eng. Comput.*, vol. 20, no. 3, pp. 314–318, 1982, doi: 10.1007/BF02442798.

[27] G. S. Stergiou et al., "Unreliable oscillometric blood pressure measurement: Prevalence, repeatability and characteristics of the phenomenon," *J. Hum. Hypertension*, vol. 23, no. 12, pp. 794–800, 2009, doi: 10.1038/jhh.2009.20.

[28] X.-F. Teng and Y.-T. Zhang, "Theoretical study on the effect of sensor contact force on pulse transit time," *IEEE Trans. Biomed. Eng.*, vol. 54, no. 8, pp. 1490–1498, Aug. 2007, doi: 10.1109/TBME.2007.900815.

[29] B. Gavish, I. Z. Ben-Dov, and M. Bursztyn, "Linear relationship between systolic and diastolic blood pressure monitored over 24 h: Assessment and correlates," *J. Hypertension*, vol. 26, no. 2, pp. 199–209, 2008, doi: 10.1097/HJH.0b013e3282f25b5a.

[30] A. M. Master and R. P. Lasser, "The relationship of pulse pressure and diastolic pressure to systolic pressure in healthy subjects, 20-94 years of age," *Amer. Heart J.*, vol. 70, no. 2, pp. 163–171, 1965.

[31] R. Mukkamala and J.-O. Hahn, "Toward ubiquitous blood pressure monitoring via pulse transit time: Predictions on maximum calibration period and acceptable error limits," *IEEE Trans. Biomed. Eng.*, vol. 65, no. 6, pp. 1410–1420, Jun. 2018, doi: 10.1109/TBME.2017.2756018.